

Adversarial Detection by Approximation of Ensemble Boundary

This work has been submitted to the IEEE for possible publication. Copyright may be transferred without notice, after which this version may no longer be accessible.

T. Windeatt

Code for this paper implementing Walsh Coefficient Examples of approximating artificial Boolean functions can be found at <https://doi.org/10.24433/CO.3695905.v1>

Abstract— A spectral approximation of a Boolean function is proposed for approximating the decision boundary of an ensemble of Deep Neural Networks (DNNs) solving two-class pattern recognition problems. The Walsh combination of relatively weak DNN classifiers is shown experimentally to be capable of detecting adversarial attacks. By observing the difference in Walsh coefficient approximation between clean and adversarial images, it appears that transferability of attack may be used for detection. Approximating the decision boundary may also aid in understanding the learning and transferability properties of DNNs. While the experiments here use images, the proposed approach of modelling two-class ensemble decision boundaries could in principle be applied to any application area.

Index Terms—Adversarial robustness, Boolean functions, ensemble, deep neural networks, machine learning, pattern analysis, spectral analysis.

I. INTRODUCTION

Despite achieving excellent performance in many application areas, Deep Neural Networks (DNNs) are known to be susceptible to being fooled. This can take many forms in various applications but visually is most striking when an image is manipulated, so that the DNN misclassifies although the required perturbation results in an image that appears no different to a human. The perturbation is computed in various ways and known as adversarial pattern generation or adversarial attack. Example images of this phenomenon can be found in [1]. Lack of susceptibility to adversarial attacks is known as adversarial robustness and is clearly a desirable property.

Besides having important practical implications, especially for security and safety-related applications the problem of adversarial attacks has been extensively studied theoretically. Indeed, there is recent recognition that adversarial pattern generation can help explain how DNNs learn, which would be helpful since there are many aspects of DNN learning which are poorly understood and remain open research questions [2]. The main idea is that an adversarial attack, which attempts to push a pattern on the other side of a decision boundary, gives a notion of how the boundary is behaving during learning.

As a result of the practical issue of the threat to DNNs, adversarial attacks and subsequent defences have become somewhat of a game. At present it appears that the attackers

are winning, since there is evidence that the current adversarial defences that claim to be robust, can all be defeated [3]. The most successful defence is adversarial training, in which the original training set is enhanced with adversarial patterns. However, the computational cost of adversarial training is such that it appears not to be practical.

Ensembles or multiple classifier systems are a well-recognised method of solving pattern recognition problems. The two main phases in ensemble design are classifier generation and combination. Classifier generation (known as individual or base classifiers) has the aim of producing accurate yet diverse classifiers, although diversity has remained an elusive concept from the early days of ensembles up to the present [4]. The combination phase is usually simple, such as a *Majority Vote* or *Weighted Vote*. Weighted combination rules have been extensively investigated but there is no established strategy for computing the weights. Trainable rules have been developed, but it is not clear whether there is any advantage and the training parameters can be difficult to set. When applied to DNNs, there is a belief that ensembles have limited usefulness, because single state-of-the-art DNNs achieve remarkable performance by themselves without the need for combining diverse individuals [25].

In this paper, an ensemble of parallel relatively weak DNNs is proposed for approximating the decision boundary using Walsh spectral coefficients. Walsh coefficients were first proposed for pattern recognition in the 1970's [5], although the assumption was that the classifier inputs were binary features rather than class labels as inputs to a combining rule. The relationship between the ensemble model in [6], described in Section II and Walsh coefficients was first established in [7], and subsequently used for ensemble pruning in [8]. In [9] it is shown that the difference between the first- and third-order coefficient approximations is a good indicator of optimal base classifier complexity. For further understanding of Walsh coefficients and their use in ensemble design see [10] [11]. Like *Majority Vote*, only class labels are used for Walsh spectral coefficients. It is shown in Section II that *Weighted Vote* is a special case of Walsh approximation.

Since interesting learning problems are ill-posed [12], some form of regularisation in the form of parameter tuning will be required. DNNs already have many parameters, and if too many parameters are introduced, the search space could become too large to be practical with parameters difficult to tune. The only parameter in the Walsh combination is the order of the Walsh coefficients, which determines how well the ensemble boundary is approximated.

T. Windeatt is with the Centre for Vision, Speech and Signal Processing, University of Surrey, Guildford GU2 7XH, UK.(email t.windeatt@surrey.ac.uk)

II. WALSH ENSEMBLES

In this paper, relatively weak *DNNs* are used as base classifiers in an ensemble that solves two-class classification problems. It is assumed that there are N parallel base classifiers, with final layer of each *DNN* providing a binary classification. Let X_m be the N -dimensional binary vector that represents the decisions of the N *DNN* classifiers for the m th pattern. If the target label for the m th pattern is denoted by Ω_m then $\Omega_m = \Phi(X_m)$ where $m = 1 \dots \mu$, $\Omega_m \in \{0,1\}$ and Φ is the unknown Boolean function that maps X_m to Ω_m . Each element of X_m represents a vertex in the N -dimensional binary hypercube.

Following [5], the discrete probability density function $p(X = X_j)$ can be approximated using Rademacher-Walsh (*RW*) polynomials as orthogonal basis functions. Therefore, in the context of an ensemble the probability of occurrence of each of the μ binary votes is computed. The *RW* polynomials contain 2^N possible terms and are formed by taking products as shown in Table I. *RW* discrete polynomial functions are orthogonal, satisfying the property that

$$\sum_{m=1}^{2^N} \varphi_j(X_m) \varphi_k(X_m) = \begin{cases} 2^N & \text{if } j = k \\ 0 & \text{if } j \neq k \end{cases} \quad (1)$$

An approximation of the discrete probability density using q basis functions and μ patterns is given by

$$\hat{p}(X) = \sum_{j=1}^q c_j \varphi_j(X) \quad (2)$$

where coefficients are given by

$$c_k = \frac{1}{2^N \mu} \sum_{i=1}^{\mu} \varphi_k(X_i) \quad (3)$$

Spectral coefficients may also be interpreted as correlation with class labels [11]. The first order coefficients, $j = 2 \dots N+1$ in Table I, represent the correlation with the class label. Second and higher order coefficients represent correlation with the logic exclusive-OR (*xor* denoted \oplus) of the respective coefficients. For example, if $j = N+2$ in Table I, the second order spectral coefficient s_{12} is given by

$$s_{12} = c_5 = \frac{1}{2^N \mu} \sum_{m=1}^{\mu} \mathcal{C}(x_{m1} \oplus x_{m2}, \Omega_m) \quad (4)$$

$$\text{where } \mathcal{C}(a, b) = \begin{cases} +1 & \text{if } a = b \\ -1 & \text{if } a \neq b \end{cases}$$

A simple example shows how to compute the three combinations of the second order contribution for a three-dimensional binary pattern $[x_1, x_2, x_3] = [0,1,1]$. With reference to Table I and (2) and (3), for $[x_1, x_2]$ the basis function is $(2x_1 - 1)(2x_2 - 1) = (-1)(1) = -1$. Similarly, for $[x_1, x_3]$ the count is -1 but for $[x_2, x_3]$ the count is +1. Adding the three contributions gives a count of -1 for that pattern. There are eight basis functions in total, the remaining being 0th, 1st and 3rd order. To compute the probability estimate of two classes ω_1, ω_0 assume prior probability is given by the number of patterns. If there are nI ω_1 patterns,

divide by nI multiplied by the eight basis functions as given in (3). After performing similar probability density estimate for ω_0 , a decision function $d(X)$ is formed by subtracting the probability estimate of the two classes, which is the probability density in (2) multiplied by prior probability:

$$d(X) = \hat{p}(X|\omega_1)p(\omega_1) - \hat{p}(X|\omega_0)p(\omega_0) \quad (5)$$

Note that the two probability estimates in (5) contain the same divisor (number of basis functions) so can be ignored when computing the decision function. The decision function based on the Walsh coefficient combiner of order y is defined as W_y , so third order is W_3 , and contains the addition of contributions from W_0, W_1, W_2 . Note from Table I that W_0 basis function ($j=1$) is constant and does not depend on the pattern elements. So W_0 is just the difference of the number of patterns in the two classes. W_1 is similar to a weighted combiner with weights set by correlation of individual classifiers with class label. In [5] [9], there is an example computation for finding the decision function using a linear approximation for a three-dimensional binary function.

A useful model for understanding ensemble behavior for two-class problems was formulated in [6], in which the assumption is made that both classes are Gaussian. The conventional wisdom is that if a classifier is too complex, achieving a very low training error rate, then the patterns under the tails of the distribution are correctly classified, leading to a decision boundary that differs from the optimal Bayes boundary, and generalises poorly. Apparently, a *DNN* can produce a decision boundary capable of correctly classifying patterns under the tail, yet still perform well on the test set. In Sec III, there is a discussion on how adversarial robustness is shedding light on this phenomenon. In [9] there is a description of how third order Walsh coefficients can be computed using the model [6].

III. ADVERSARIAL ROBUSTNESS

Adversarial examples were first demonstrated in [13] [14]. In this paper, the focus is limited to adversarial robustness, as applied to images. The intention of an adversarial attack is to perturb an image so that it is misclassified, yet to the human eye appears little or no different. It is an interesting topic theoretically, because it shows the limitations of machine learning applied to images, particularly for *DNNs* when using Backpropagation. From a practical standpoint, for an application that is safety or security related a misclassification could incur a high cost e.g. a self-driving car, that misclassifies a pedestrian. It is not obvious why human invisible adversarial perturbations provide a successful attack. However, perhaps it is not surprising because *DNNs* generally learn using Backpropagation, which is not biologically plausible. Indeed, some have questioned whether a different learning algorithm would need to be developed, more in line with the way humans learn [15].

In the context of images, there are many theories as to why *DNNs* are not robust to adversarial pattern generation. In [16], authors argue that gradient-based optimisation requires *DNN*

> REPLACE THIS LINE WITH YOUR MANUSCRIPT ID NUMBER (DOUBLE-CLICK HERE TO EDIT) <

classifiers to be designed to be sufficiently linear, and that this local linearity causes susceptibility to adversarial examples and the transference to different classifiers. The theoretical analysis in [17] identifies fundamental bounds on the susceptibility of a classifier to adversarial attacks, and concludes that adversarial examples may be inevitable. The analysis in [18], links adversarially robust generalisation to over-fitting, arguing that depending on the particular dataset distribution, more data may be needed. In [19], by improving the robustness to random noise, a relationship between robustness and curvature of the decision boundary is established, suggesting that geometric constraints on the curvature of the decision boundary should be imposed.

Many theories, either explicitly or implicitly through the data distribution, link adversarial robustness to the decision boundary. Other theories relate robustness to features rather than geometric perspective [20]. For example, in [21], features in the final layer of the *DNN* are shown to be split into robust and non-robust features, the former being aligned with the visual features used by humans. Although there are many theories of why *DNNs* are not adversarially robust, the focus here is on the boundary theory. The main hypothesis here is that decision boundaries with high curvature allow adversarial perturbations to be found, but change the curvature of the decision boundary, which is then approximated in a different way by Walsh coefficients compared to the clean images.

Adversarial defences have in some cases been based upon ensembles, such as [22] [23] [24]. The consensus at present, appears to be that ensembles do not provide defences that cannot be broken by adaptive attacks [1] [3] [25]. Walsh ensemble is different in that a complex boundary can be approximated by much simpler classifiers. This is demonstrated in [9] for the artificial 2D circular dataset problem, in which simple individual classifiers under-fit, yet *W3* provides a good approximation to the optimal Bayes boundary, while *Majority Vote* and *W1* do not.

As explained in Section II, the model in [6] includes the overlapping area under the tail of the distribution that contains those patterns that would be fit by a *DNN* with low or zero error. In the conventional view, this would give rise to overfitting, negatively impacting generalisation. Yet *DNNs* achieve low or zero error on these patterns while maintaining good generalisation. A possible reason is that high curvature of decision boundaries enables the patterns to be correctly classified, with boundaries such that other test error patterns in the vicinity are not mis-classified. Imagine that each pattern in the overlap area is correctly classified via its own highly curved, possibly disconnected boundary. If the boundary is very tight, it would not affect generalisation, yet could be easily perturbed to mis-classify. The visualisations of highly curved decision boundaries in [2] [19] suggest that this may be the case. The difficulty is that the space is high-dimensional and there is no guarantee that 2D visualisations are giving a true picture. It is better perhaps to think of it as a tool to try to help understand in an intuitive sense the reason for the relationship between accuracy and robustness.

Experiments described in Section IV are based on checking adversarial detection for several adversarial attacks (*ADVs*) that use a variety of attack methods. The *ADVs* considered were

Carlini-Wagner, *ElasticNet*, *HopSkipJump*, *Zeroth Order Optimization*, along with the five chosen below and all described in [26]. In Section IV, *dog/cat(d/c)* is chosen as the most difficult *CIFAR10* [27] problem in terms of error rate. The following *ADVs* used for experiments in Section IV and implemented in [26], were chosen based on their attack success on the *d/c* dataset with default parameters selected: *Deepfool (DF)* [30], *Projection Gradient Descent (PG)* [31], *Universal Adversarial Perturbation (UA)* [32], *Fast Gradient Sign Method (FG)* [16], *Basic Iterative Method (BI)* [33]. While it was possible to increase attack success of the *ADVs* by increasing perturbation levels, the attacks generally produced noticeable visual distortion of the images.

Following [1], *ADVs* may be classified according to attacker goal, knowledge and strategy. The goal is targeted vs untargeted, the former referring to an attack aimed at misclassifying a specified class, while the latter allows any misclassification. Normally multi-class problems are assumed, but since only two class problems are considered in this paper, the attack is targeted, which is a more difficult problem [34] as evidenced by the choice of attacks discussed in the previous paragraph. Attacker knowledge is either white box or black box. White box assumes that the attacker has complete knowledge of the classifier and parameters, while black box relies on the transferability of attack images produced by a classifier that is in general different from the target classifier. All attacks considered in Section IV are white box. Attacker strategy is split into additive noise and geometric distortions (such as rotation and translation to induce misclassifications). All attacks considered here rely on additive noise, either using optimisation algorithms (*PG*, *DF*, *UA*) or simpler and faster sensitivity analysis to determine the contribution of each input feature, for example gradient descent or Jacobian matrix.

According to [1] adversarial defences are based on input transformation, adversarial detection or by design. A defence based on Walsh approximation would be considered an adversarial detection approach. The most similar approach is the adversarial detection technique in [29], which is based on finding a classification score threshold and is distinguished from classifier and input data modification defences.

IV. EXPERIMENTAL EVIDENCE

A. Datasets and classifiers

Various two-class problems were chosen according to difficulty from *CIFAR10* [27], *dog/cat (d/c)*, *truck/auto(t/a)*, *horse/deer(h/d)*, *frog/cat(f/c)*, *deer/bird(d/b)* and from *MNIST* digit recognition [28] 9/4, 7/2, 9/7, 8/5, 8/3. For *CIFAR10*, the input RGB images are 32x32, and for *MNIST*, the grey-level images are 28x28.

The experiments are designed to test the hypothesis that a Walsh coefficient approximation of an ensemble boundary allows a relatively weak *DNN* classifier combination to detect adversarial images. The architecture consists of the following twenty layers, with the first layer replaced by 28x28 for *MNIST*: $32 \times 32 \times 3$ images/32 3×3 convolutions with stride [1 1] and padding 'same'/ReLU/32 3×3 convolutions with stride [1 1] and padding [0 0 0 0]/ ReLU/2x2 max pooling with stride [2 2] and padding [0 0 0 0]/25% dropout/64 3×3

> REPLACE THIS LINE WITH YOUR MANUSCRIPT ID NUMBER (DOUBLE-CLICK HERE TO EDIT) <

convolutions with stride [1 1] and padding same/ReLU/64 3×3 convolutions with stride [1 1] and padding [0 0 0 0]/ReLU/ 2×2 max pooling with stride [2 2] and padding [0 0 0 0]/25% dropout/ Flatten activations into 1-D / 512 fully connected layer/ReLU/50%dropout/2 fully connected layer /Softmax /Classification Output.

Training uses gradient descent with *adam* optimiser. The ensemble has twenty-one base classifiers, since it was found experimentally that increasing the number beyond twenty-one did not improve or decrease performance for the datasets and number of training patterns considered here. The diversity in each base classifier of the ensemble is due to random starting weights and drop-out.

Classifier parameters were selected based on *d/c*, which is the most difficult two-class problem in *CIFAR10*, and then fixed for testing other two-class problems. The main parameters to set are the number of training epochs, number of nodes in the final layer and the drop-out rate. These were selected as 30, 512 and 50 percent respectively. It was found that varying the number of epochs/nodes and drop-out rate did not significantly alter performance.

B. Experimental Results for DNN ensemble

The nomenclature for this section is as follows: *ADV*s *DF,PG,UA,FG,BI* are defined in Section III and use default parameters as given in [26], except that for *FG,BI* a value of twenty is used for epsilon. The Walsh coefficient order W_y is defined in Section II, and *CIFAR10* and *MNIST* problems are defined in Section IV A. *TE* and *TR* refer to the clean test and training images, respectively, while *ADVTE* and *ADVTR* refer to the adversarial perturbed images e.g. *DFTR* refers to *DeepFool(DF)* training images. Class 1 and 2 are abbreviated as *cl1* and *cl2*, so for example *TEcl1* refers to class 1 of the clean test images. Note that *TEcl1* is compared with *ADVcl2* since both *TE* and *ADV* images are predicted class 1. Similarly *TEcl2* is compared with *ADVcl1*. The goal of adversarial detection is to maximise both the percentage of *TE* images accepted, denoted *TEACC* and the percentage of *ADV* images rejected, denoted *ADVREJ*.

All Figures show results for *d/c*, with class 1 as *dog*, class 2 as *cat*. In order to achieve the most reliable results for *TEACC* and *ADVREJ*, both *TR* and *TE* are split such that the clean image is retained if correctly classified by *Majority Vote*. Similarly each *ADV* is split so that the image is retained if incorrectly classified. Initially, for training the classifiers the full training set is used, and then the Walsh coefficient computation is reported for the split images.

Fig. 1(a) shows ensemble *TRcl1* and *DFTRcl2* average error vs order of Walsh coefficient for a twenty-one classifier ensemble. Fig. 1(b) is similar to Fig. 1(a), showing error for *TRcl2* and *DFTRcl1*. Figs. 2(a)(b) show the equivalent to Fig. 1 for Walsh decision probability. Note that for Figs. 1(a)(b) the W_1 *TR* error is 0 while *DFTR* error is 100 percent, since the dataset was split as explained above.

Figs. 2(c)(d) show Walsh decision probability for *TE* vs *ADVTE* for all five *ADV*s. For *TEcl1* vs *ADVcl2* Figs 2(a)(c)

show that Walsh probability is generally lower for *ADVcl2* with higher oscillations from odd to even coefficients. For *TEcl2* vs *ADVcl1* Figs. 2(b)(d) show that Walsh probability is generally lower for *ADVcl1* and oscillations not as noticeable. Curves of *ADV*s in comparison with *TE* shown in Figs. 2(c)(d) show similar trends to Figs. 2(a)(b) indicating that transferability across classifiers trained on *ADV*s can be used to detect adversarial images.

From Figs. 2 (c) (d) there are various measures that could be used to potentially detect *ADV*s. For the set of experiments presented in this paper the second order coefficient (W_2) and the change from first to second order (W_1/W_2) is chosen for each dataset and each class. The difference between *TE* and *ADV* in Figs. 2 (c) (d) is an average, and in order to determine whether the difference can be used to detect *ADV*s, Fig. 3(a) shows a typical *TEACC/ADVREJ* curve as the W_1/W_2 detection threshold is varied. A pattern is accepted if greater than probability threshold. The optimal threshold which gives 87% for *TEcl1/DFcl2* would need to be determined, but has not been investigated here. If *TR* was used to find optimal threshold, *TEcl1/DFcl2* would be 86/91%. In practice, by using a validation set values should be somewhere between 87/87 and 86/91. By varying the threshold it would be possible to alter the trade-off, for example from Fig. 3(a) *DFREJ* = 100% could potentially be achieved at *TEACC* = 80%.

Tables II-V show *TEACC* and *ADVREJ* for all problems considered from *CIFAR10* and *MNIST*. Numbers in the tables are italicised to indicate that W_2 is chosen rather than W_1/W_2 . No entry in the tables occurs when there too few patterns that have been successfully attacked for a reliable estimate.

Table II shows the optimal *TEACC/ADVREJ* for all datasets in *CIFAR10* using *TEcl1/ADVcl2* and *TEcl2/ADVcl1*. Table III shows the values of *TEACC/ADVREJ* if the threshold is set by *DF* (for all datasets except *f/c*). From Table III it may be observed that the optimal thresholds for each *ADV* are similar, indicating that transferability of attack across classifiers is not strongly dependent on the particular attack. Table IV shows the optimal values if *Majority Vote* is used for *TEcl1/ADVcl2*. In comparison with Table II, the averages are much lower and there is much more variability among the different *ADV*s.

Table V shows the equivalent results for *MNIST* for *TEcl1/ADVcl2* and *TEcl2/ADVcl1*. However this is an easier dataset allowing perfect separation so that the optimal *TEACC/ADVREJ* of 100/100 for both class 1 and 2 may be obtained for all problems. The entries show the lower probability threshold and range over which both *TEACC* and *ADVREJ* are greater than 98 percent. It may be seen that the initial probability thresholds are very similar with high probability range (from 0.12 to 0.38 for *TEcl1/ADVcl2* and .15 to .52 for *TEcl2/ADVcl1*), indicating that it should be possible to locate the optimal *TEACC/ADVREJ*.

Finally, Fig. 3(b) shows *TR* and *TE* ensemble error using the full training/test set. For higher order Walsh, *TR* error goes to zero while *TE* error increases, showing the capability of Walsh coefficients to learn *TR* perfectly, but not generalising well.

V. DISCUSSION

In practice most adversarial defences have been shown to fail assuming enough is known about defence details. Further work is required to determine how difficult it is to defeat a defence based on approximating an ensemble decision boundary using Walsh coefficients. It is not yet possible to describe such a defence as effective, since there has been no attempt to defeat it using an adaptive attack, that is one which is specifically designed to overcome the Walsh defence. A suggested way of overcoming such a defence is to design a loss function based on all classifiers in the ensemble, as discussed in [3], for the ensemble defences [23][24]. Even if an adaptive attack is successful, it is still hoped that using Walsh coefficient approximation will provide a tool that provides more insight into the training and transferability of *DNN* classifiers. A significant finding of this study is that transferability measured by Walsh approximation is very similar across different adversarial attacks. Also for two-class problems the two classes may show different transferability properties. Further investigation is needed to understand the relationship between transferability and correlation as measured by the Walsh approximation.

While the experiments here use images, the proposed approach of modelling two-class ensemble decision boundaries could in principle be applied to any application area. The analysis in this paper is restricted to two-class problems, but it may be easier to understand *DNNs* using two-class, before considering the more complex multi-class case. From a practical standpoint, it should be possible to scale the approach to multi-class using *Error-Correcting-Output-Codes (ECOC)* [24], which reduces multi-class problems to two class. Overall, further study is warranted into using Walsh ensembles to model a decision boundary formed from *DNNs* for adversarial robustness and for understanding *DNN* transferability and learning.

REFERENCES

- [1] A. Serban, E. Poll, and J. Visser, "Adversarial Examples on Object Recognition: A Comprehensive Survey," *ACM Comp. Surveys*, Vol. 53 Issue 3, June 2020, Art. No. 66.
- [2] G. Ortiz-Jiménez, A. Modas, S. M. Moosavi-Dezfooli, and P. Frossard, "Optimism in the Face of Adversity: Understanding and Improving Deep Learning through Adversarial Robustness," *Proceedings of the IEEE*, vol. 109, no. 5, pp. 635-659, May 2021.
- [3] F. Tramèr, N. Carlini, W. Brendel, and A. Madry, "On Adaptive Attacks to Adversarial Example Defenses," *Proc. NeurIPS*, Vancouver, Canada, 2020, pp. 1633-1645.
- [4] T. Windeatt, "Accuracy/diversity and ensemble MLP classifier design," *IEEE Trans. Neural Netw.*, vol. 17, no. 5, pp. 1194-1211, Sep. 2006.
- [5] J.T Tou and R. C. Gonzales, *Pattern Recognition Principles*, Addison-Wesley, 1974, pp. 151-4.
- [6] K. Tumer and J.Ghosh, "Error correlation and error reduction in ensemble classifiers" *Connection Science*, vol. 8, no. 3, pp. 385-404, 1996.
- [7] T. Windeatt and C. Zor, "Minimising Added Classification Error Using Walsh Coefficients," *IEEE Trans. Neural Netw.*, vol. 22, no. 8, pp. 1334-1339, Aug. 2011.
- [8] T. Windeatt and C. Zor, "Ensemble pruning using spectral coefficients", *IEEE Trans. Neural Netw. Learn. Syst.*, vol. 24, no. 4, pp. 673-678, 2013.
- [9] T. Windeatt, C. Zor and N. C. Camgoz, "Approximation of Ensemble Boundary Using Spectral Coefficients," *IEEE Trans. Neural Netw. Learn. Syst.*, vol. 30, no. 4, pp. 1272-1277, April 2019.
- [10] T. Windeatt, "Vote Counting Measures for Ensemble Classifiers," *Pattern Recognition*, vol. 36, no. 12, pp. 2743-2756, 2003.
- [11] L. Hurst, D. M. Miller, and J. Muzio, *Spectral Techniques in Digital Logic*, Academic Press, NY, USA, 1985.
- [12] A. N. Tikhonov and V. A. Arsenin, *Solutions of Ill-posed Problems*, Washington, DC, USA: Winston & Sons, 1977.
- [13] C. Szegedy et al., "Intriguing properties of neural networks", [arXiv:1312.6199v4](https://arxiv.org/abs/1312.6199v4), Feb. 2014.
- [14] B. Biggio et al., "Evasion attacks against machine learning at test time", *Proc. ECMLPKDD*, Lecture Notes in Computer Science, vol 8190. Springer, Berlin., https://doi.org/10.1007/978-3-642-40994-3_25
- [15] F. Lin, " Learning in Neural Networks: Feedback-Network-Free Implementation and Biological Plausibility," *IEEE Trans. Neural Netw. Learn. Syst.* vol. 33, no. 12, pp. 7888 – 7898, Dec. 2022.
- [16] L. J. Goodfellow, J. Shlens, and C. Szegedy, "Explaining and harnessing adversarial examples", [arXiv:1412.6572v3](https://arxiv.org/abs/1412.6572v3) Mar., 2015.
- [17] A. Shafahi, W. Huang, C. Studer, S. Feizi, and T. Goldstein. "Are adversarial examples inevitable?", [arXiv:1809.02104v3](https://arxiv.org/abs/1809.02104v3) Feb. 2020.
- [18] L. Schmidt, S. Santurkar, D. Tsipras, K. Talwar, and A. Madry. "Adversarially robust generalization requires more data", *Proc. NeurIPS*, Montreal, Canada, Dec. 2018.
- [19] A. Fawzi, S. Moosavi-Dezfooli, and P. Frossard, "Robustness of classifiers: from adversarial to random noise", *Proc. NeurIPS*, Barcelona, Spain, Dec. 2016.
- [20] C. Zhang, P. Benz, C. Lin, A. Karjauv, J. Wu and I. S. Kweon, "A Survey On Universal Adversarial Attack", [arXiv:2103.01498v2](https://arxiv.org/abs/2103.01498v2) Jan. 2022.
- [21] A. Ilyas, S. Santurkar, D. Tsipras, L. Engstrom, B. Tran, and A. Madry, "Adversarial Examples are not Bugs, they are Features", *Proc. NeurIPS*, Vancouver, Canada, Dec. 2019
- [22] T. Pang, K. Xu, C. Du, N. Chen, and J. Zhu, "Improving adversarial robustness via promoting ensemble diversity", *Proc. ICML*, Calif., USA, June, 2019.
- [23] S. Sen, B. Ravindran, and A. Raghunathan. "Ensembles of mixed precision deep networks for increased robustness against adversarial attacks". [arXiv:2004.10162v1](https://arxiv.org/abs/2004.10162v1) Apr. 2020.
- [24] G. Verma and A. Swami, "Error correcting output codes improve probability estimation and adversarial robustness of deep neural networks", *Proc. NeurIPS*, Vancouver, Canada, Dec. 2019.
- [25] W. He, J. Wei, X. Chen, N. Carlini, and D. Song. "Adversarial example defense: Ensembles of weak defenses are not strong", *Proc. Workshop on Offensive Technologies*, Vancouver, BC, Canada, 2017.
- [26] M. Nicolae et al., Adversarial Robustness Toolbox, [arXiv:1807.01069v4](https://arxiv.org/abs/1807.01069v4) <https://adversarial-robustness-toolbox.readthedocs.io/en/latest/>
- [27] A. Krizhevsky, CIFAR-10 dataset, [Online]. Available: <https://www.cs.toronto.edu/~kriz/cifar.html>.
- [28] Y. LeCun, MNIST dataset, [Online]. Available: <http://yann.lecun.com/exdb/mnist/>
- [29] H. Kwon, Y. Kim, H. Yoon, D. Choi, "Classification score approach for detecting adversarial example in deep neural network", *Multimedia Tools and Applications*, vol. 80, pp. 10339-10360, Mar. 2021.
- [30] S. Moosavi-Dezfooli, A. Fawzi, P. Frossard A. Krizhevsky, "DeepFool: A Simple and Accurate Method to Fool Deep Neural Networks", *Proc. CVPR*, Las Vegas, USA, June 2016, pp. 2574-2582.
- [31] A. Madry, A. Makelov, L. Schmidt, D. Tsipras, and A. Vladu, "Towards deep learning models resistant to adversarial attacks", [arXiv:1706.06083v4](https://arxiv.org/abs/1706.06083v4) Sept. 2019.
- [32] S. Moosavi-Dezfooli, A. Fawzi, O. Fawzi, and P. Frossard, "Universal adversarial perturbations" *Proc. CVPR*, Hawaii, July 2017, pp.1765-1773.
- [33] A. Kurakin, I. Goodfellow, and S. Bengio., "Adversarial examples in the physical world", *Artificial Intelligence Safety and Security*, Chapman and Hall, 2018.
- [34] A. Aldahdooh, W. Hamidouche, S. A. Fezza and O. Déforges, "Adversarial example detection for DNN models: a review and experimental comparison", *Artificial Intelligence Review*, volume 55, 2022, pp 4403-4462.

> REPLACE THIS LINE WITH YOUR MANUSCRIPT ID NUMBER (DOUBLE-CLICK HERE TO EDIT) <

TABLE I
RADEMACHER-WALSH POLYNOMIAL FUNCTIONS

j	$\varphi_j(x)$
1	1
2	$2x_1 - 1$
\vdots	\vdots
$N + 1$	$2x_N - 1$
$N + 2$	$(2x_1 - 1)(2x_2 - 1)$
\vdots	\vdots
$N + 2 + N(N - 1)/2$	$(2x_{N-1} - 1)(2x_N - 1)$
$N + 2 + N(N - 1)/2$	$(2x_1 - 1)(2x_2 - 1)(2x_3 - 1)$
\vdots	\vdots
2^N	$(2x_1 - 1)(2x_2 - 1) \dots (2x_N - 1)$

TABLE II
CIFAR10 OPTIMAL *TEACC/ADVREJ*
TECL1/ADVCL2 | *TECL2/ADVCL1*

<i>Pro</i>	<i>DF</i>	<i>PG</i>	<i>UA</i>	<i>FG</i>	<i>BI</i>
d/c	87 93	85 94	90 87	85 86	85 85
t/a	93 93	89 94	--- 95	91 94	85 94
h/d	94 92	96 91	96 -	96 79	95 78
f/c	--- 94	--- 92	--- 95	95 93	93 93
d/b	91 94	91 95	92 --	93 92	92 94
Ave	91 93	90 93	93 92	92 89	90 89

TABLE III
CIFAR10 OPTIMAL *TEACC/ADVREJ* USING PROBABILITY
THRESHOLD FROM ADV (SHOWN BOLD)
TOP 5 ROWS *TECL1/ADVCL2*, BOTTOM 5 ROWS *TECL2/ADVCL1*

<i>Pro</i>	<i>DF</i>	<i>PG</i>	<i>UA</i>	<i>FG</i>	<i>BI</i>
d/c	87	85/85	86/99	85/85	86/84
t/a	93	93/71	-	93/78	91/55
h/d	94	94/98	94/98	94/98	94/96
f/c	-	-	-	95	95/90
d/b	91	91/91	90/100	91/98	91/97
d/c	93	93/95	86/98	87/85	86/84
t/a	93	93/99	94/97	93/96	93/95
h/d	92	91/91	-	78/88	75/90
f/c	94	94/90	94/99	94/92	94/92
d/b	94	94/99	-	94/91	94/94

TABLE IV
CIFAR10 OPTIMAL *TECL1/ADVCL2* USING *MAJORITY VOTE*

<i>Pro</i>	<i>DF</i>	<i>PG</i>	<i>UA</i>	<i>FG</i>	<i>BI</i>
d/c	74	55	85	65	70
t/a	90	85	-	85	80
h/d	82	60	55	75	72
f/c	-	-	-	85	80
d/b	80	70	77	84	80
Ave	81	67	72	79	76

TABLE V
MNIST PROBABILITY/RANGE MULTIPLIED BY 100
FOR GREATER THAN *TEACC/ADVREJ* OF 98/98 PERCENT
TOP 5 ROWS: *TECL1/ADVCL2*, BOTTOM 5 ROWS *TECL2/ADVCL1*

<i>Pro</i>	<i>DF</i>	<i>PG</i>	<i>UA</i>	<i>FG</i>	<i>BI</i>
9/4	2/12	2/12	3/12	2/13	2/13
7/2	5/24	5/25	5/24	5/24	5/25
9/7	62/38	62/38	62/38	62/38	62/38
8/5	8/37	8/37	-	6/38	8/37
8/3	7/28	7/28	7/34	7/28	7/28
9/4	9/15	9/15	8/22	9/15	9/15
7/2	6/39	7/35	4/61	6/39	6/44
9/7	6/32	6/32	-	5/32	5/34
8/5	48/52	48/52	48/52	48/52	48/52
8/3	4/20	3/21	4/20	4/20	4/21

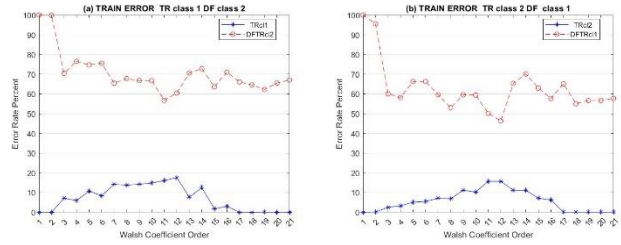


FIG. 1 TRAIN ERROR VS WALSH COEFFICIENT ORDER (A) TRAIN CLASS DOG ADV CLASS CAT (B) TRAIN CLASS CAT ADV CLASS DOG

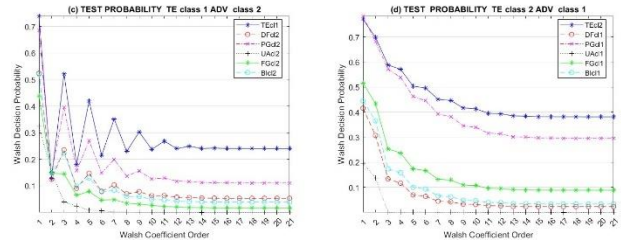
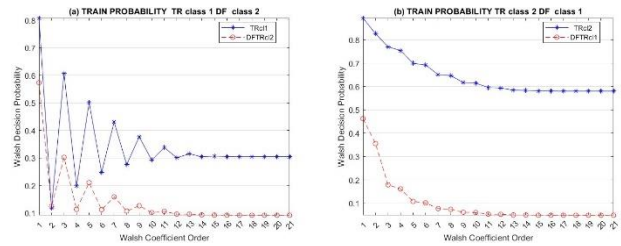


FIG. 2 WALSH DECISION PROBABILITY VS WALSH COEFFICIENT ORDER (A) TRAIN CLASS DOG DF CLASS CAT (B) TRAIN CLASS CAT DF CLASS DOG (C) TEST CLASS DOG ADV CLASS CAT (D) TEST CLASS CAT ADV CLASS DOG

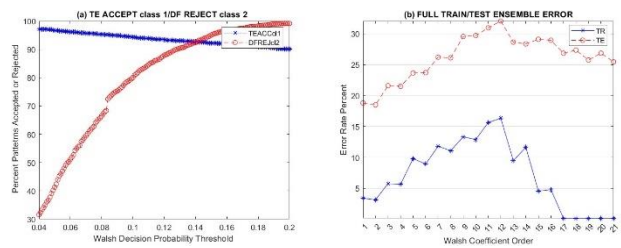


FIG. 3 (A) PERC. OF CLEAN TEST IMAGES ACCEPTED FOR *DOG* AND *DF* ATTACK IMAGES REJECTED FOR *CAT* AS DETECTION THRESHOLD IS VARIED (B) ENSEMBLE ERROR OF *DOG/CAT* VS ORDER OF WALSH COEFFICIENT